Sixth International Symposium on Turbulence and Shear Flow Phenomena
Seoul, Korea, 22-24 June 2009

THE INFLUENCE OF A MULTIPLE-HARMONIC PULSATILE WAVEFORM ON THE SECONDARY FLOW IN A CURVED TUBE

Chekema Prince
Department of Biomedical Engineering,
Polytechnic Institute of New York University
6 Metrotech Center, Brooklyn, NY 11201
chekema.prince@gmail.com

Sean D. Peterson
Department of Mechanical and Mechatronics Engineering
University of Waterloo
200 University Avenue West, Waterloo, Ontario, Canada N2L 3G1
peterson@mme.uwaterloo.ca

Michael W. Plesniak
Department of Mechanical and Aerospace Engineering
The George Washington University
801 22nd Street NW, Academic Center, Suite 739, Washington DC 20052
plesniak@gwu.edu

ABSTRACT

Under the application of a harmonically oscillating pressure gradient of sufficiently high frequency, the dominant secondary flow pattern in a curved tube exhibits inward centrifuging. The present study investigates the spatial and temporal evolution of the secondary flow structure in a curved tube driven by a physiologically-inspired pulsatile waveform. Specifically, the study seeks to address whether an inward centrifuging secondary flow structure (Lyne-type vortices) is possible with a nominally low-frequency input waveform. Experimental data were acquired using Laser Doppler Velocimetry (LDV). Experimental results show that fully developed flow is established after negotiating approximately 150° of the 1/7 radius to radius of curvature bend arc. In the developing region, Lyne-type vortices are observed to develop spatially along the curved pipe. At the peak of the input waveform, these vortices develop near the outer wall of the bend 90° from the bend entrance and become more centralized downstream. At the fully developed region the Lyne-type vortices become prominent within the cross-section of the bend. Temporally, the Lyne-type vortices are observed to develop near the outer wall during the acceleration phases of the waveform, become centralized at the peak of the waveform, and move back toward the outer wall during the deceleration phases. Emergence of complex secondary flow structures at low oscillation frequencies may have applications in low speed mixing and in stent design.

INTRODUCTION

It is well established that steady flow in curved tube develops a centrifugal instability that can amplify and result in secondary flows. These secondary flows are characterized by counter-rotating, outwardly centrifuging vortices (Dean vortices). In standard Dean vortices, the flow in the center of the tube moves outwards, away from the center of the radius of curvature of the bend then recirculates back along the walls of the tube (see Figure 1a). The secondary flow physics is governed by the Dean number, D, which represents the ratio of the square root of the product of the inertia and centrifugal force to the viscous force (Berger et al., 1983). The Dean number is defined as

$$D = \mathrm{Re}\left(\frac{a}{R}\right)^{\frac{1}{2}} \tag{1}$$

where a is the pipe radius, R is the radius of curvature, and Re is the Reynolds number. The Reynolds number is defined as

$$\mathrm{Re} = \frac{2a\overline{W}_0}{\nu} \tag{2}$$

where $\overline{W}_0$ is the mean axial velocity and ν is the kinematic viscosity.

When flow in the same bend undergoes zero-mean harmonic oscillation, however, entirely different flow patterns are possible. Lyne investigated this problem via a perturbation analysis using the Stokes' layer thickness as the perturbation parameter (Lyne, 1971). Interestingly, Lyne found that when the radius of the tube is large compared with the Stokes' layer thickness, that is when the viscosity is confined to a small region near the walls, the “inviscid core” in the center of the tube experiences *inward* centrifuging.

The inward centrifuging in the inviscid core is a consequence of the flow in the Stokes' layer, which rotates in same sense as the vortices in the steady flow case, dragging the fluid at the interface between the two zones. Lyne's analysis is confined to large frequencies and experimental observation has found inward centrifuging occurs at dimensionless frequency parameters, α, (Womersley number) greater than 12 (Sudo et al. 1992). The Womersley number is defined as

$$\alpha = a\left(\frac{\omega}{\nu}\right)^{\frac{1}{2}} \tag{3}$$

where ω is the angular frequency of the driving oscillations. The Womersley number can be viewed as a ratio of unsteady inertial forces to viscous forces. At low Womersley values ($\alpha < 10$) the viscous forces dominate unsteady inertial forces and the driving pressure and velocity waveform are nearly in phase (Ku, 1997). At high Womersley values, the unsteady inertial forces dominate resulting in a lag between the driving pressure and the velocity waveforms since the fluid tends to maintain its current direction despite a change in the driving pressure force.

The conditions prompting the transition from Dean to Lyne vortices are studied numerically by Dennis and Ng (1982). They develop numerical solutions of the Navier Stokes equations for steady flow in a curved pipe over the range D = 135 – 7071 by transforming the governing PDEs into an infinite series of ODEs using a Fourier series substitution, then truncating and solving the finite set of equations. They report their numerical solution to converge to a two-vortex solution (Dean vortices) for Dean numbers up until D = 1351. Above this Dean number both a two- and four-vortex solutions are observed. Above D = 1351 the solution (secondary flow structure) depends on the imposed initial conditions. Axial velocity profiles for the two-vortex solution show the maximum velocity occurring on the axis of symmetry. In contrast, twin maxima symmetrically placed with regard to the axis of symmetry are observed for the four-vortex solution.

Using numerical and experimental methods, Sudo et al. (1992) investigate the secondary flow patterns in fully-developed, laminar, zero-mean sinusoidal flow. Experimental measurements are made in a helical pipe 450° from the bend entrance and used to validate numerical solutions. Sudo et al. classify the secondary flow patterns in 5 categories shown in Figure 1. The categories are labeled as (I) Dean circulation (Figure 1a), (II) deformed Dean circulation (Figure 1b), (III) intermediate between Dean and Lyne circulations (Figure 1c), (IV) deformed Lyne circulation (Figure 1d) and (V) Lyne circulation (Figure 1e).

Intermediate circulation between Dean and Lyne circulations (Figure 1c) is observed for D = 200 - 345 at $\alpha >$ 10, in which the pressure force exceeds the centrifugal force in the central region. A stagnation region that forms near the outer wall in previous stages moves toward the inner wall and small Lyne vortices appear near the outer wall for a short period during the cycle (Type IIIB). As α and D are increased the Lyne vortices become centralized and are present for the entire cycle (Figure 1d).

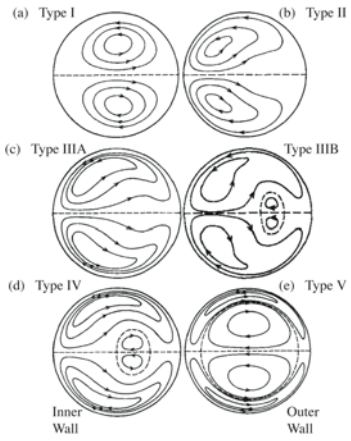

Figure 1. Five classifications of secondary flow structure for zero-mean harmonic forcing. Adapted from Sudo et al. (1992).

Boiron et al. (2007) reports on the spatial development of the secondary flow structure along the length of the curved pipe and the dependence on the slope of the deceleration phases of the input waveform. They use hot-film measurements and numerical simulations based on the experimental geometry to model unsteady flow in a curved tube for a Dean number range of D = 110 – 420 and Womersley number range of α = 8 – 21. Their tube has a radius to radius of curvature ratio of 0.073 and the input waveforms mimic the systolic phase of the cardiac cycle, which is defined as the ventricular ejection time. At $\alpha \approx 8$, two input waveforms with similar acceleration slopes and Dean numbers that differed by a factor of 2 induce Dean vortices within the cross-section of the bend. The input waveform with a greater deceleration slope induces the development of Lyne vortices in the developing region of the flow 90° from the bend entrance.

The numerical simulations of Boiron et al. (2007) confirm that differences in the relative magnitudes of the centrifugal force and the force due to the radial pressure gradient determine the direction of fluid motion along the x-axis, that is, from the inner to outer wall. At the onset of acceleration, the centrifugal force is greater than the radial pressure gradient and drives the fluid towards the outer wall indicating a standard Dean vortex configuration. Towards the peak of the waveform, as the rate of acceleration begins to decrease, the centrifugal force and the radial pressure gradient are balanced except near the inner wall where the centrifugal force dominates. During deceleration, the radial pressure gradient dominates and the fluid moves toward the inner wall, suggestive of the formation of Lyne vortices. Qualitatively, the sum of the centrifugal force, the force due to the radial pressure gradient, and the inertial forces is approximately zero in the central region of the tube substantiating the "inviscid core" description of this region.

In the present study, experiments are used to determine whether secondary flow patterns presumed to occur only at high frequencies can be generated at a nominally low

frequencies by employing a complex driving waveform consisting of multiple harmonic contributions.

EXPERIMENTAL SETUP

A simple schematic of the experimental setup used in this study is shown in Figure 2. The working fluid is pumped from the reservoir into the entrance pipe leading to the curved test section by an Ismatec Programmable Gear pump with a magnetically driven Micropump A-mount pump head. A time-varying voltage signal is supplied to the Ismatec pump via a National Instruments 68-pin *E Series* 16 channel DAQ card connected to a PC. National Instruments *LabView 6.1* software with a custom virtual instrument applies the desired voltage waveform to the pump. For further details, see Peterson and Plesniak (2008). Figure 2 also shows the coordinate system defined for the setup. The x-axis points toward the center of the radius of curvature, the z-axis points in the stream-wise direction and the y-axis is formed using the standard right hand convention. The angle of the measurement plane, θ, increases from the entrance of the bend to the exit of the bend and sweeps through 180° total.

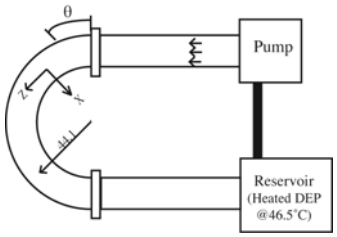

Figure 2. Experimental setup

A glass tube measuring 1.2 m long by 12.6 mm diameter by 1.2 mm wall thickness precedes the test section and ensures fully developed flow entering the test section (Ku, 1997). The test section consists of a 180° bend formed from two machined and polished Plexiglas pieces fused together. The ratio of tube radius to radius of curvature is 1/7. This ratio is selected because of its prevalence in previous literature on pulsatile flow through curved geometries, see for example Swanson et al. (2006). The Plexiglas bend is attached to the entrance/exiting glass tubes using silicon caulk. The bend is fixed to a rigidly-mounted Plexiglas base to provide stability and accurate positioning of the measurement equipment.

Working Fluid

Diethyl phthalate (DEP) is chosen as the working fluid for this experiment based on previous research indicating its appropriateness for *in vitro* cardiovascular models (Miller et al., 2006). DEP is a commonly used plasticizer in industrial applications. It has a high index of refraction (n = 1.501), low dynamic viscosity (13.024 mPa·s), is safe to use, and is relatively inexpensive (Alpha Aesar- 2.5kg = $39.20) (De Lorenzi et al., 1997; Miller et al., 2006).

To match the index of refraction of the Plexiglas bend, the index of refraction of the DEP is reduced to 1.491 by heating the fluid. De Lorenzi et al. (1997) report various DEP properties measured as functions of temperature, including index of refraction. Interpolation of their results indicate that at a temperature of 46.5° C (319.5 K) the index of refraction of DEP matches that of the plexiglas test section. At this temperature, the DEP has a kinematic viscosity and density of 4.7636 (10^{-6} $m^2 \cdot s^{-1}$) and 1.0948 ($g \cdot cm^{-3}$), respectively.

The DEP temperature is maintained by placing the fluid in a one-gallon paint can that is in turn placed in a heated circulating water bath. A temperature difference of 5° C is measured between the DEP in the reservoir and at the exit of the test section. To account for the temperature loss at the measurement location, the DEP reservoir is held at a temperature of approximately 51 +/- 1° C. Changes in fluid properties due to a 1°C change in temperature are: $n \approx 2.68 * 10^{-2}$ %; kinematic viscosity ≈ 2.74%; density ≈ $7.76*10^{-2}$%. All pipes leading to the test section are insulated to reduce heat loss.

Laser Doppler Velocimetry (LDV)

Laser Doppler Velocimetry (LDV) is used to measure the velocity at discrete points within the experimental apparatus. The LDV system used in this experiment is a one-component Dantec Dynamic Flow Lite 1D system operating in burst mode. Silvered glass spheres of 18μm and corresponding particle Stokes number of 0.01 are added to the working fluid (Peterson and Plesniak, 2008). The velocity sampling rate is 300 – 800Hz. Higher sampling rates are obtained at the center of the bend cross-section. Measurements are acquired in 1 mm increments along the x and y axes at every 15° along the bend. At θ = 165° velocity measurements are acquired throughout the cross-section to determine the stream-wise profile in the full-developed region of the bend.

Input Waveform

The input waveform used in these experiments is based on ultrasound and ECG measurements by Holdsworth et al. (1997) of blood flow within the left and right carotid arteries of 17 healthy volunteers, see Figure 3 for the general form. The waveform is characterized by increased volumetric flow during the systolic phase when the blood is ejected from the heart. The dicrotic notch, which reflects the cessesation of systole, occurs at the minimum volumetric flow. The diastolic phase begins after the dicrotic notch and continues until the end of the waveform period. The Reynolds number values for the waveform, based upon the vessel diameter of 6.4mm, the viscosity and density of blood of 3.5cP and 1060 kg/m respectively, range from 24 to 1424 with a mean value of 364. The Reynolds number is based on the diameter of the vessel and the mean axial velocity. The Womersley value for the waveform is 4.6.

Peterson and Plesniak (2008) scaled the *in vivo* waveform for use in a cardiovascular model in which the working fluid was water by matching the Reynolds and Womersley numbers. The flow rate was scaled by the Reynolds number, while the period of the waveform was scaled to match the Womersley value based on the density and viscosity of water. A similar scaling procedure is used in this study to obtain the proper velocity and period for the DEP in the current experimental setup.

The first 15 harmonics of the Fourier decomposition of the volumetric flow waveform are used to compute the centerline velocity waveform for the straight entrance pipe

from the Womersley solution (Womersley, 1955). The Fourier decomposition shows that the waveform is largely formed from the first 6 harmonics, though the higher harmonics are necessary to properly fit the systolic portion of the waveform. In other words, the acceleration and deceleration portion of the systolic peak depend on the higher harmonics.

Figure 3 displays the Womersley solution for the velocity at the center point of the entrance pipe (U_{cp}) and the corresponding acceleration waveform. The period of the velocity waveform using DEP as the working fluid could not be scaled to match the Womersley value of 4.6 reported by Holdsworth due to difficulty matching the measured centerline velocity waveform to the centerline velocity waveform determined by the Womersley solution. This is believed to be caused by a limitation of the pump since the gear pump cannot operate in reverse and the inertia of the fluid keeps the fluid moving when the pump is stopped. This causes a mismatch between the desired waveform and the measured waveform during the deceleration phases. The Womersley value of 3.6 is used instead, corresponding to a waveform period of 4.0 seconds. At the lower Womersley number the match between the experimental data and the Womersley solution is within 15%.

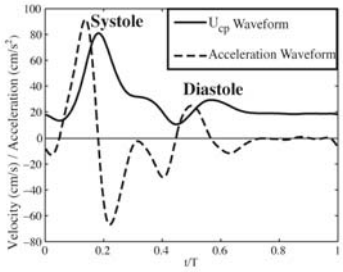

Figure 3. Womersley solution for the velocity at the center-point of the entrance pipe (U_{cp}) and the corresponding acceleration waveform.

Prior to each measurement within the bend, a time-trace of the velocity at the straight pipe centerline approximately 5D upstream of the bend entrance is acquired to confirm that the driving waveform is correct. Overall, the centerline velocity over the period of the waveform shows good qualitative agreement with the theoretical centerline velocity derived from the Womersley solution determined from the physiological waveform.

A quantitative assessment of the agreement between experimental measurements at the centerline within the straight pipe and the Womersley solution is determined by calculating the percent difference between the two waveforms. Eleven straight pipe measurements are averaged in order to perform the percent error calculation. The maximum error during the deceleration phase of the primary peak is 15%, which occurs at t/T = 0.2639. The overall absolute maximum deviation value is ~6.30 cm/s, which equates to an error of 20% in the dicrotic notch. Despite the large deviations at the phases mentioned, the error generally remains below 10% for the rest of the phases.

RESULTS

Axial Skew

As the fluid moves through the bend, the curvature results in axial skew, that is, higher values of the stream-wise velocity toward the outer or inner wall of the pipe. Axial skew is influenced not only by the Dean number but also by the acceleration and deceleration of the flow input waveform. The stream-wise velocity profile is observed to skew toward the inner wall at the entrance of the bend due to streamline curvature then shifts toward the outer wall further downstream as the centrifugal forces overcome the radial pressure gradient.

The stream-wise velocity profile for the present driving waveform is shown in Figure 4 for four different phases, corresponding to the acceleration phase of the systolic peak, maximum velocity, deceleration of the systolic peak, and maximum velocity of the diastolic peak at θ = 165° (See Figure 2 for the measurement location).

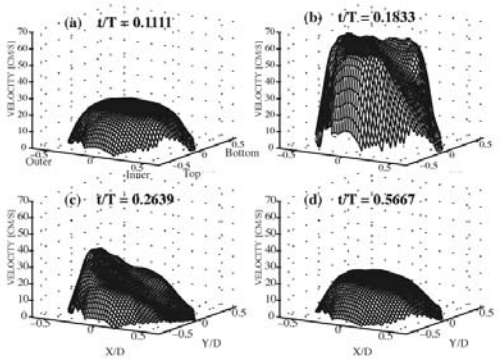

Figure 4. Stream-wise velocity at θ = 165° at various phases

During acceleration, as the Reynolds number increases (Figure 4a), the velocity profile is similar to plug flow. During deceleration (Figure 4b and c), the profile skews toward the outer wall of the bend. This is hypothesized to occur due to the impact of the adverse pressure gradient during the deceleration phases more strongly influencing the fluid near the inner wall, which has less inertia in comparison with the fluid near the outer wall of the bend. This creates a "chair-like" shape of the surface plot at t/T = 0.1833, corresponding to the peak Reynolds number value. This persists until the flow starts to accelerate again and the profile returns to a more uniform shape (Figure 4d).

Secondary Flow

Cross-stream measurements are obtained within the cross-section of the bend in order to assess the development of secondary flow. Evaluation of vortex formation within the cross-section is based only on the V_x component of the velocity. Velocity measurements in the x-direction are acquired along the x and y axes of the cross-section. The left hand column of Figure 5 presents contour plots of V_x during the systolic phases of the waveform at various angles along the bend. The abscissa of each contour plot in Figures 5 is the dimensionless time, t/T, during the systolic phase of the input waveform shown in Figure 3. The ordinate of each contour plot is the position along the y-axis from the "top" to the "bottom" of the tube. Thus, a vertical slice through any contour yields the cross-stream velocity profile at that particular phase. Positive velocity values (indicated by solid lines in the contour) represent fluid motion toward the inner

wall while negative velocity values (indicated by dotted lines in the contour) represent fluid motion toward the outer wall. Based on these measurements and previous studies on secondary flow development in curved pipes, a schematic of the possible vortex structures is determined for each measurement angle and phase of the driving waveform.

Standard Dean vortices are characterized by counter-rotating vortices carrying fluid from the inner wall to the outer wall of the bend along the x-axis, which is represented as negative values of the velocity (dotted contour lines) in the center of the contour plot. The fluid returns to the inner wall along the top and bottom wall of the tube, which is represented as positive values (solid contour lines) near y/D = ±0.5 in the contour plots. Positive velocities at the top and bottom walls, along with negative velocities in the central region along the y-axis are prominent at most phases in Figure 5, indicating that the secondary flow structure is usually Type I (refer to Figure 1 for flow types).

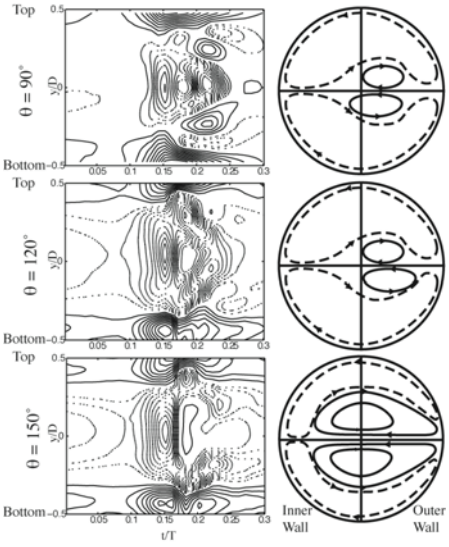

Figure 5. Contour plots of V_x along the y-axis of the tube at various locations and the corresponding spatial development of Lyne vortices at t/T = 0.1833

As discussed previously, Lyne vortices rotate in the opposite direction to Dean vortices and carry fluid from the outer wall toward the inner wall in the central region of the cross-section. When Lyne vortices exist, the Dean type vortices are pushed toward the "top" and "bottom" walls of the bend, that is, into the Stokes layer. The formation of Lyne vortices is identified in the contour maps as positive velocity (solid lines) at the "top" and "bottom" walls as well as along the tube centerline. The positive velocity regions are separated by negative velocity regions.

The position and prominence of Lyne vortices are observed to change temporally and spatially in the developing region of the tube and temporally in the fully developed region. By focusing on a fixed time in the pulse cycle, the spatial development of vortices can be observed along the bend. At the velocity maximum (t/T = 0.1833), a change is observed in the secondary flow structure, in which a second inner vortex pair is produced, similar to Lyne vortices. The development of Lyne vortices at this phase at D ≈ 538 corresponds to the observations made by Sudo et al. (1992) at higher Dean numbers but α = 18 - 28. Combining velocity magnitude and directional information with the vortex structure data in Sudo et al. (1992), the right hand column of Figure 5 is constructed to represent the likely vortex structure at t/T = 0.1833 for each spatial location. Spatial development along the bend can be observed by comparing the three subfigures depicting θ = 90°, 120°, and 150°, where θ is defined in Figure 2 as the measurement angle from the entrance of the bend to the exit of the bend. Lyne vortices are observed to develop near the outer wall at θ = 90°. From θ = 90° to 120°, the Lyne vortices move toward the center of the cross-section and become prominent and centralized by θ = 150°. The vortex structure at t

A schematic of the temporal development of secondary flow in the fully developed region of the bend (θ = 150°) is shown in Figure 6 based on the contour map shown in Figure 5.

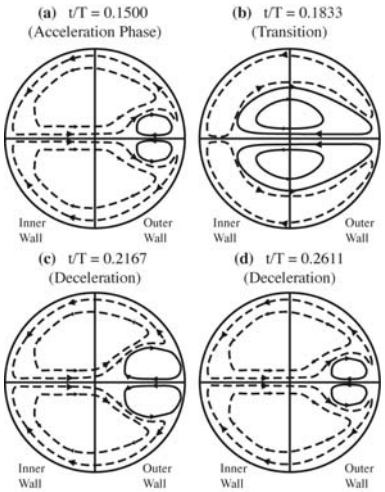

Figure 6. Temporal development of Lyne vortices at θ = 150° during the systolic peak.

At t/T = 0.1500, during the acceleration phase of the input waveform, small Lyne vortices appear near the outer wall and push the prominent Dean vortices toward the top and bottom walls (Figure 6a). At the transition between the acceleration and deceleration phases, t/T = 0.1833, the Lyne vortices become prominent within the cross-section (Figure 6b). As previously discussed, the Stokes layer, where the centrifugal effects are confined, host the Dean-type vortices during this "inertial" portion of the flow cycle. The centrifugal effects propel the fluid in the inviscid core toward the outer wall of the pipe. This fluid returns to the inner wall of the pipe along the horizontal centerline thus forming the Lyne-type vortices in the center region of the cross-section. During the deceleration phase, t/T = 0.2167, the Lyne vortices decrease in size and move back toward the outer wall (Figure 6c) and the Dean vortices once again become prominent. As the deceleration phase progresses, the Lyne vortices near the outer wall are observed to further decrease in size, though they seem to persist throughout the rest of the waveform as very small vortices near the outer wall (Figure 6d).

The vortex formations observed at $\theta = 150°$ can be classified using the five categories of Dean vortices reported by Sudo et al. (1992). At t/T = 0.1500, the vortex formation can be classified as type (III), which is intermediate between Dean and Lyne circulations. For type (III) classification, Sudo et al. state that the pressure gradient is superior to the centrifugal force in the central region. In addition, stagnant fluid near the outer wall moves toward the inside. The small Lyne vortices near the outer wall are said to appear at certain periods of the waveform cycle and eventually move toward the inner wall. Type (V) Lyne circulation is observed at t/T = 0.1833 where viscous effects are restricted to a thin Stokes layer near the wall as the Lyne-type vortices occupy the central region. The vortex formation returns to a Type (III) formation, with the additional twin vortices near the outer wall at t/T = 0.2167 and t/T= 0.2611.

CONCLUSIONS

Previous studies investigating unsteady flow in a curved tube have shown that Dean vortices are predominant at low Womersley number. Unsteady flow at a high Womersley number ($\alpha \geq 12$) has been shown to cause the development of a near-wall Stokes layer that can subsequently lead to the development of Lyne vortices within the cross-section of the bend. These previous studies have largely focused on input waveforms consisting of a single sinusoid. The development of Lyne vortices at the low Womersley number of 3.6 in this study is atypical, as the flow should be entirely viscously dominated. The observed Lyne vortex formation is likely due to the higher harmonics that compose the input waveform and the influence of the acceleration/deceleration rates of the waveform.

The multiple harmonics that compose the input waveform represent a range of Womersley numbers rather than a single Womersley number as in studies using simple harmonic waveforms. Around the peak of the waveform (t/T = 0.1833) where Lyne vortices appear prominent within the cross-section of the bend, the “local” Womersley value for these phases is considerably higher than the “global” Womersley value of 3.6 for the entire waveform. The strong influence of the higher harmonics (i.e. high Womersley number) around the peak of the waveform induces Lyne vortices and corroborates the observed development of Lyne vortices in the literature. The results presented here show the development of Lyne vortices is not only restricted to high frequency single harmonic waveforms or steady flow at high Dean number values but can be induced by a multiple harmonic waveform during phases in which the impact of higher harmonics is the greatest.

In additional to the fluid dynamics observations discussed, DEP was proven a viable option as a working fluid in cardiovascular models. The index of refraction and viscosity can be easily adjusted by changing the temperature of the fluid. The ability to adjust the index of refraction by changing the temperature is valuable in the reduction of measurement errors in optical systems caused by mismatched index of refraction between the cardiovascular model material and the working fluid.

FUTURE WORK

The investigation of fluid motion in curved pipes under the influence of complex waveforms is directly applicable to the study of blood flow through the human vasculature and the study of vascular disease. The secondary flow development observations in this study can serve as a baseline to study the impact of stent implantation in arteries. Stents implantation is often used to treat arterial stenosis, which causes the narrowing to the blood vessel lumen. The stent acts as scaffolding to restore the vessel lumen to its native diameter. It is hypothesized that stent implantation may disrupt the formation of vortices within the cross-section of blood vessels in the vascular system. The impact of stent struts can be determined by comparing the development of secondary flow for various strut dimensions and spacing with the secondary flow development observed in the current study.

ACKNOWLEDGEMENTS

Supported by NSF Grant CBET #0729995

REFERENCES

Alpha aesar products., 2008, from http://www.alfa.com/

Berger, S. A., Talbot, L., & Yao, L. S. (1983). Flow in curved pipes. *Annual Review of Fluid Mechanics, 15*(1), 461-512.

Boiron, O., Deplano, V., & Pelissier, R. (2007). Experimental and numerical studies on the starting effect on the secondary flow in a bend. *Journal of Fluid Mechanics, 574*, 109-129.

De Lorenzi, L., Fermeglia, M., & Torriano, G. (1997). Density, refractive index, and kinematic viscosity of diesters and triesters. *Journal of Chemical & Engineering Data, 42*(5), 919-923.

Dennis, S. C. R., & Ng, M. (1982). Dual solutions for steady laminar flow through A curved tube. *Q J Mechanics Appl Math, 35*(3), 305-324.

Holdsworth, D. W., Norley, C. J., Frayne, R., Steinman, D. A., & Rutt, B. K. (1999). Characterization of common carotid artery blood-flow waveforms in normal human subjects. *Physiological Measurement, 20*(3), 219-240.

Ku, D. N. (1997). Blood flow in arteries. *Annual Review of Fluid Mechanics, 29*(1), 399-434.

Lyne, W. H. (1971). Unsteady viscous flow in a curved pipe. *Journal of Fluid Mechanics, 45*(1), 13-31.

Miller, P., Danielson, K., Moody, G., Slifka, A., Drexler, E., & Hertzberg, J. (2006). Matching index of refraction using a diethyl phthalate/ethanol solution for in vitro cardiovascular models. *Experiments in Fluids, 41*(3), 375-381.

Peterson, S., & Plesniak, M. (2008). The influence of inlet velocity profile and secondary flow on pulsatile flow in a model artery with stenosis. *Journal of Fluid Mechanics, 616*, 263-301.

Sudo, K., Sumida, M., & Yamane, R. (1992). Secondary motion of fully developed oscillatory flow in a curved pipe. *Journal of Fluid Mechanics, 237*, 189- 208.

Womersley, J. R. (1955). Method for the calculation of velocity, rate of flow and viscous drag in arteries when the pressure gradient is known. *The Journal of Physiology, 127*(3), 553-563.